RSC Advances

PAPER

View Article Online
View Journal | View Issue

Cite this: *RSC Adv.*, 2023, **13**, 25939

Synthesis of biofuel precursors from benzaldehyde and cyclopentanone *via* aldehyde–ketone condensation in a deep eutectic solvent system

Yunqi Cao, [ab] Fang Liu,[a] Yunyun Liu *[b] and Qiang Yu[c]

Production of biofuel precursors from biomass-derived platform compounds (BDPC) has a profound influence on biofuel industries. Herein, an efficient catalytic system composed of the deep eutectic solvent (DES, *i.e.*, ChCl/Fa) and $SnCl_4$ (ChCl/Fa–$SnCl_4$) was developed to produce biofuel precursors (C12 and C19) through aldehyde–ketone (A–K) condensation of benzaldehyde (BD) and cyclopentanone (CPO). ChCl/Fa–$SnCl_4$ exhibited the prospective catalytic performance and given the high selectivity (S_{C12} = 49.20%, S_{C19} = 15.20%) and total yield ($Y_{C12+C19}$ = 64.37%) of C12 and C19, as well as 99.96% BD conversion under the optimized conditions (BD : CPO molar ratio of 1 : 6, ChCl : Fa molar ratio of 1 : 12, 4 mmol $SnCl_4$, 80 °C for 120 min). Subsequently, the C12 and C19 precursors were successfully applied to generate cyclic alkanes ($C_{12}H_{14}$ and $C_{19}H_{18}$) by hydrodeoxygenation with selectivity of 37.61% and 24.10%, respectively. Finally, the potential catalytic mechanism was explored by density functional theory (DFT) calculations. The results unveiled that the formation of a stable structure for the ChCl/Fa–$SnCl_4$ system was ascribed to the viable interactions among ChCl, Fa and $SnCl_4$ by coordination bonds, electrostatic interactions and H-bonds, which decreased reaction energy barriers and drove the condensation of BD and CPO. In this case, the catalytic reactions between BD and CPO were enhanced to promote the synthesis of C12 and C19. This work provides a novel strategy for the applicability of different BDPC to synthesize fuel precursors for the development of liquid biofuels.

Received 16th June 2023
Accepted 10th August 2023

DOI: 10.1039/d3ra04058e

rsc.li/rsc-advances

Introduction

The global energy demand, which is anticipated to exceed 28% by 2040, imperatively necessitates the development of more renewable biofuels, such as bio-jet fuels, bioethanol, biobutanol and biodiesel, *etc.*[1–3] Sustainable liquid biofuels (SLB) attained from biomass-derived platform compounds (BDPC) have drawn tremendous attention due to the concerns of the energy crisis and the goals of "carbon peaking" and "carbon neutrality".[4–6] With the advantages of renewability, low toxicity, low sulfur content, biodegradability and high-octane number, SLB can serve as a promising alternative fuel to fossil fuels to be compatible with existing engines for different applications.[7,8]

Normally, BDPC (aldehydes, alcohols, phenols, *etc.*) can be directly converted into biofuel precursors by the C–C coupling strategies, such as aldol condensation, hydroxyalkylation/alkylation (HAA), Michael addition, benzoic condensation, Robinson annulation, *etc.*, followed by hydrogenation or hydrodeoxygenation (HDO) to synthesize SLB with carbon numbers of C8–C22.[9–12] Huang *et al.* successfully synthesized a biodiesel precursor (C15) from biomass-derived furfural and 2-methylfuran through a HAA reaction.[13] However, biofuel precursors are typically hydrocarbons with short carbon chains, low density and calorific value, and poor low-temperature fluidity, which cannot well meet the requirements of transportation fuels owing to the light molecules of BDPC with only 5 or 6 carbon atoms.[7,14] The elongation of carbon chains is an accessible and cost-effective way to upgrade the quality of biofuel precursors, and the biofuels will have higher density and efficiency after introducing naphthenic or aromatic hydrocarbons.[15]

Benzaldehyde (BD), as the most commonly used aromatic aldehyde in industry, has been recommended as a potential fuel resource to synthesize valuable fuels and chemicals by C–C coupling and HDO or hydrogenation.[16,17] Wang *et al.* synthesized biofuel 2-methylfuran through the selective hydrogenation of BD and furfural with the highest yield of 78.4% under mild conditions.[18] Aldehyde–ketone (A–K) condensation reaction as one of the cornerstones of synthetic chemistry is an organic synthesis reaction with important applications in the fine chemical and pharmaceutical industries. It can increase the length of carbon chains through C–C coupling to connect aldehyde and carbonyl groups, which needs to be carried out in the presence of catalysts.[19–21] For example, the bio-jet fuel

[a]*School of Low-Carbon Energy and Power Engineering, China University of Mining and Technology, Xuzhou 221116, China*
[b]*College of Mechanical and Electrical Engineering, Shaanxi University of Science & Technology, Xi'an 710021, China. E-mail: liuyu282009@126.com*
[c]*Institute of Biomass Engineering, South China Agricultural University, Guangzhou 510642, China*

precursors (C7–C14) derived from BDPC (furfural, butyraldehyde, acetone, and butanone) were produced by A–K condensation using a bifunctional catalyst.[22] The catalysts usually applied in A–K condensation include solid acid catalysts (TiO_2, zeolites, *etc.*),[6,15] homogeneous and heterogeneous basic catalysts (NaOH, $Ca(OH)_2$, CaO, and hydrotalcite, *etc.*),[22,23] and bifunctional catalysts (Sn-MFI, $MgF_{2-x}(OH)_x$, *etc.*), *etc.*[24,25] These catalysts are conducive to the effective conversion of BDPC for the production of high-quality biofuels. However, the solid-phase heavy components are primarily formed in A–K condensation process, resulting in the deactivation of most catalysts due to the deposition of the components on the surface of catalysts.[15,22] Furthermore, the actual applications for developing renewable biofuels from BDPC are restricted due to the complex separation, difficult recovery, corrosion of equipment and environmental pollution by effluent of these catalysts.[1,3,22] Thus, the green and high-efficiency catalysts are imperatively desired as a prerequisite for the synthesis of biofuels.

Deep eutectic solvents (DESs) composing of hydrogen bond donor (HBD) coupled with hydrogen bond acceptor (HBA) has been extensively applied as a green organic solvent with easy preparation, low cost, good biodegradability and biocompatibility, high solvation capability and specific active sites for superior synthesis of SLB and fine chemicals.[1,2,26,27] DESs used in biomass conversion and biofuel synthesis primarily consist of acids (formic acid, lactic acid, oxalic acid, *etc.*), bases (choline chloride, betaine, atropine, *etc.*), alcohols (glycerol, urea, menthol, ethylene glycol, *etc.*) and metal salts ($ZnCl_2$, $SnCl_4$, NaCl, *etc.*) based on the differences between HBDs and HBAs.[1,6,28–30] DESs prepared by coupling choline chloride (ChCl) and carboxylic acids have been found to be an exceptional alternative to convert BDPC into biofuel precursors.[3,31] In addition, metal chlorides ($NiCl_2$, $CrCl_3$, $SnCl_4$, *etc.*) were reported to have a cooperative effect with DESs to act as the aldose isomerization and condensation reactions of BDPC.[32–34] Guo *et al.* developed a cheap and elegant DES (ChCl–$CrCl_3$) converting glucose into 5-hydroxymethylfurfural (HMF) with over 70% yield.[34] Tin tetrachloride ($SnCl_4$), recognized as a prevalent, inexpensive and tractable Lewis acid with low toxicity, can serve as an efficient catalyst to convert biomass-derived carbohydrates into value-added chemicals.[32,35,36] Hu *et al.* found that the combination of $SnCl_4$ and ionic liquids ([EMim]BF_4) was efficiently suitable for converting glucose into HMF with the yield of 61%.[32]

Previous work demonstrated that fuel precursors (C10 and C15) could be synthesized by the condensation of furfural and cyclopentanone in DES ChCl/Fa combined with $SnCl_4$ catalytic system.[37] However, the selectivity and carbon chains extension of the fuel precursors were still deficient, and the catalytic mechanism lacked also a profound understanding at the molecular level. The aim of this work was to further upgrade the selectivity and carbon chain length of fuel precursors *via* A–K condensation and reveal the catalytic mechanism of the DES system. Hence, the DES system (ChCl/Fa–$SnCl_4$) was formed to catalyze A–K condensation of BD and CPO for synthesizing fuel precursors. Subsequently, the HDO reaction was carried out to produce cyclic alkane fuels from the biofuel precursors. Eventually, the condensation process of BD and CPO and the possible mechanism of the catalytic system were specifically investigated by density functional theory (DFT). Our findings provide a competitive strategy for the conversion of BDPC into biofuel precursors to product sustainable liquid biofuels.

Experimental

Materials

Benzaldehyde (BD), cyclopentanone (CPO, 99.5%), formic acid (Fa), choline chloride (ChCl), $SnCl_4 \cdot 5H_2O$ (abbreviated as $SnCl_4$ in the following), dichloromethane (CH_2Cl_2) and Ru/C (Ru 5%) catalyst were purchased from Shanghai Macklin Biochemical Co., Ltd (Shanghai, China). Methanol was purchased from Tianjin Fuyu Fine Chemical Co, Ltd (Tianjin, China). All reagents were analytical reagent and used without further purification. The deionized water used was produced in the laboratory.

Preparation of biofuel precursors

The DES ChCl/Fa was prepared by water bath heating. Specifically, ChCl and Fa were added to a 500 mL beaker in certain molar ratios (ChCl : Fa = 1 : 4, 1 : 8, 1 : 12, 1 : 16 and 1 : 20, respectively) and then placed in a water bath at 60 °C with a magnetic stirring (150 rpm) for 30 min. The synthesis of cyclic biofuel precursors by A–K condensation of BD and CPO was carried out in a 75 mL pressure-resistant bottle (P17002, Synthware) using oil bath heating. BD and CPO with different molar ratios (BD : CPO = 1 : 3, 1 : 6, 1 : 9 and 1 : 12, respectively) were dissolved in the DESs, and then $SnCl_4$ was added as catalyst. The reaction was subjected to a specified temperature with a magnetic stirring speed of 500 r min^{-1} for a certain period of time. After the reaction, the samples were taken out and cooled, and then were diluted with methanol and CH_2Cl_2 respectively for subsequent analysis.

Hydrodeoxygenation (HDO) of biofuel precursors

The HDO of biofuel precursors was carried out in a 100 mL stainless steel autoclave (CHEMN, Anhui, China). In each group of experiments, 30 mL of biofuel precursors and 15 mL of water–methanol mixture (molar ratio was 1 : 1) used to provide hydrogen by methanol aqueous phase reforming (MAPR) were placed in the autoclave, and then 1.5 g of 5% Ru/C powder was added to the system as catalyst. The temperature was heated from room temperature to 200 °C at a heating rate of 5 °C min^{-1}. The agitator speed of the reaction kettle was maintained at 300 rpm. The reaction lasted for 6 h after reaching the predetermined temperature and the reaction pressure was autogenous pressure. After the reaction, the autoclave was cooled to room temperature, and the products were diluted with methanol and CH_2Cl_2 to a certain multiple respectively for subsequent analysis. In this study, control variates were applied to guide the experiments and all experiments were performed in triplicate with the average value reported.

Analysis methods of products

Qualitative analysis of products diluted with methanol was performed using a Gas Chromatography-Mass Spectrometer

(GC-MS, TRACE 1300ISQ) equipped with a DM-5MS column (30 m × 0.25 mm × 0.25 μm). The helium gas with a split ratio of 50 : 1 was used as the carrier gas, and the energy of ion source was 70 eV. The air flow of injector was 64.50 mL min^{-1}, and the inlet and detector temperatures were 250 °C and 320 °C, respectively. Temperature programming: firstly, set the program temperature to be 60 °C of insulation 2 min, then rise to 210 °C with a heating rate of 10 °C min^{-1}, finally rise to 270 °C with a heating rate of 5 °C min^{-1}.

Quantitative analysis of products diluted with CH_2Cl_2 was conducted using a Gas Chromatograph (GC, GC-2010 PLUS, SHIMADZU) with the same column type and size as GC-MS. Air, nitrogen and hydrogen were used as the carrier gas with the gas pressures of 0.6 MPa, 0.6 MPa and 0.4 MPa respectively. The temperature procedure was the same as that of GC-MS. The quantification of products was determined by the self-contained integration method of GC system. The corrected and integrated peak area obtained in the GC system represented the relative content of products.

Calculation of products

The conversion, selectivity and yield of products were calculated using the following formulas (1)–(6):

$$C_{BD} = \frac{n_1}{n_0} \times 100\% \quad (1)$$

$$S_{C12} = \frac{n_2}{n_1} \times 100\% \quad (2)$$

$$S_{C19} = \frac{n_3}{n_1} \times 100\% \quad (3)$$

$$Y_{C12} = C_{BD} \times S_{C12} \quad (4)$$

$$Y_{C19} = C_{BD} \times S_{C19} \quad (5)$$

$$Y_{C12+C19} = C_{BD} \times S_{C12+C19} \quad (6)$$

where, C_{BD} is the conversion of BD, n_0, n_1, n_2 and n_3 are the moles of initial BD, converted BD, BD converted to C12 and C19, respectively; S_{C12} and S_{C19} are the selectivity of C12 and C19, respectively; Y_{C12}, Y_{C19} and $Y_{C12+C19}$ are the yield of C12, C19 and C12 + C19, respectively.

DFT calculations

DFT calculations were conducted to get insight into the plausible catalytic mechanism of this condensation process and the interaction between DES ChCl/Fa and $SnCl_4$ under the DMol^3 module using Materials Studio software (Accelrys Materials Studio 2020, San Diego, CA, USA). Reactants (BD and CPO), DES ChCl/Fa, $SnCl_4$, and products (C12, C19 and H_2O) were constructed in 3D Atomistic document and the arrangements of atoms positions were optimized by the "clean" tool. Geometry optimization task of all structures was undertaken by the B3LYP functional using TS custom method for DFT-D parameters while the convergence tolerance of energy, maximum force and displacement was set at 1.0×10^{-6} Ha, 0.002 Ha $Å^{-1}$ and 0.005 Å, respectively. The self-consistent field (SCF) tolerance was set at 1.0×10^{-6} Ha with the DNP 4.4 basis set and the searing energy was set as 0.005 Ha. The dielectric constant was set to 78.54 using water as solvation model. Other parameters were set as default.

Results and discussion

Production of biofuel precursors from BD

Table 1 presents the main product compounds of BD and CPO condensation observed from the GC-MS spectrum (Fig. 1). The biofuel precursors of 2-benzylidene-cyclopentanone (C12) and 2,5-dibenzylidenecyclopentanone (C19) with higher relative abundance (88.16 and 95.37, respectively) were successfully developed by the condensation of BD and CPO in ChCl/Fa–$SnCl_4$ system. The reaction pathways for the condensation to form C12 and C19 precursors were supposed to be a two-stage condensation process as shown in Fig. 2. It is speculated that BD firstly reacted with CPO to form the primary product C12 precursor and remove a molecule of H_2O in the initial stage of the condensation, and then the generated C12 continued to condense with CPO to form the secondary product C19 precursor. This process demonstrated the biofuel precursors can be prepared by A–K condensation of BD and CPO in a ChCl/Fa–$SnCl_4$ system.

Effect of temperature and time on biofuel precursors

Fig. 3 showed the effect of temperature and time on the production of C12 and C19 precursors. It can be observed from

Table 1 Components of condensation products

Number	Residence time (min)	Peak width	Relative abundance	Compound
(1)	1.53	0.09	83.50	Formic acid
(2)	3.15	0.08	78.67	Cyclopentanone
(3)	5.63	0.30	76.92	Benzaldehyde
(4)	6.51	0.07	41.37	(1-Methylbutyl)-cyclopentanone
(5)	12.17	0.07	75.23	2-Cyclopentylidene-cyclopentanone
(6)	15.71	0.18	88.16	2-Benzylidene-cyclopentanone
(7)	18.11	0.25	27.30	5,7-Dimethyl-2,3-dihydroinden-1-one
(8)	19.69	0.07	20.88	Dibutyl phthalate
(9)	29.09	0.47	95.37	2,5-Dibenzylidenecyclopentanone

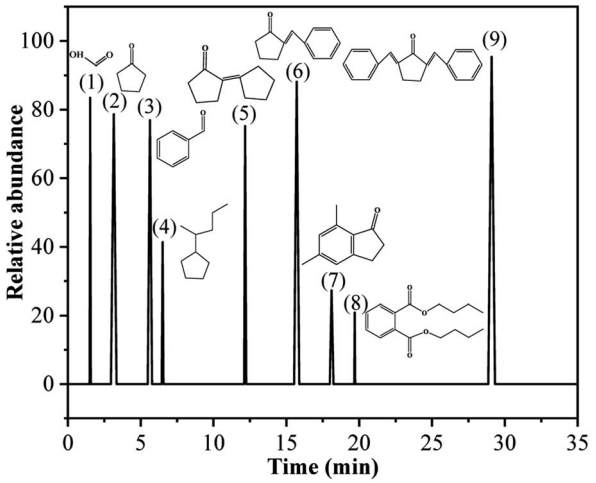

Fig. 1 GC-MS spectrum of the condensation products of BD and CPO.

Fig. 3a that the conversion of BD and the selectivity of C12 and C19 were lower when the temperature was 60 °C, and C_{BD}, S_{C12}, S_{C19} and $Y_{C12+C19}$ were 78.25%, 8.39%, 6.46% and 11.62%, respectively. The conversion of BD increased to nearly 100% with the temperature increasing from 80 °C to 120 °C, indicating that the condensation efficiency can be enhanced by increasing the reaction temperature. S_{C12} and S_{C19} initially increased and then decreased with increasing temperature from 60 °C to 120 °C. The selectivity of C12 and C19 increased significantly when the temperature increased from 60 °C to 80 °C, with the S_{C12}, S_{C19} and $Y_{C12+C19}$ increased by 49.20%, 15.20% and 64.37%, respectively compared with 60 °C. It was observed from Fig. 3 that S_{C12} decreased significantly (22.63%) and the S_{C19} increased slightly (19.25%) at 100 °C. These results showed that the increase of temperature can improve the selectivity of BD directional condensation to C12 and C19, and high temperature may facilitate the further conversion of C12 to C19. However, the S_{C12} at 120 °C increased slightly (53.23%) compared with that at 80 °C, but no condensation of C19 at this time. This reason may be that, on the one hand, the high-temperature condensation at 120 °C destroyed the hydrogen bonds between Fa and ChCl in DES, which weakened the solvent effect and catalytic action of the DES. On the other hand, it may be attributed to the evaporation of Fa (the boiling point is 100.8 °C) that changed the status of the reaction system, which reduced the acidity of the system and the effect of mass and heat transfer of the substrates during the condensation process.[20,21]

It was found from Fig. 3b that C12 and C19 did not condense successfully although BD was almost completely converted

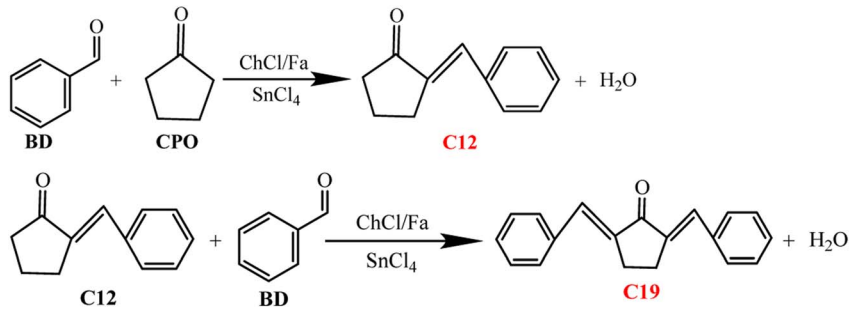

Fig. 2 Reaction pathways for the formation of C12 and C19 precursors.

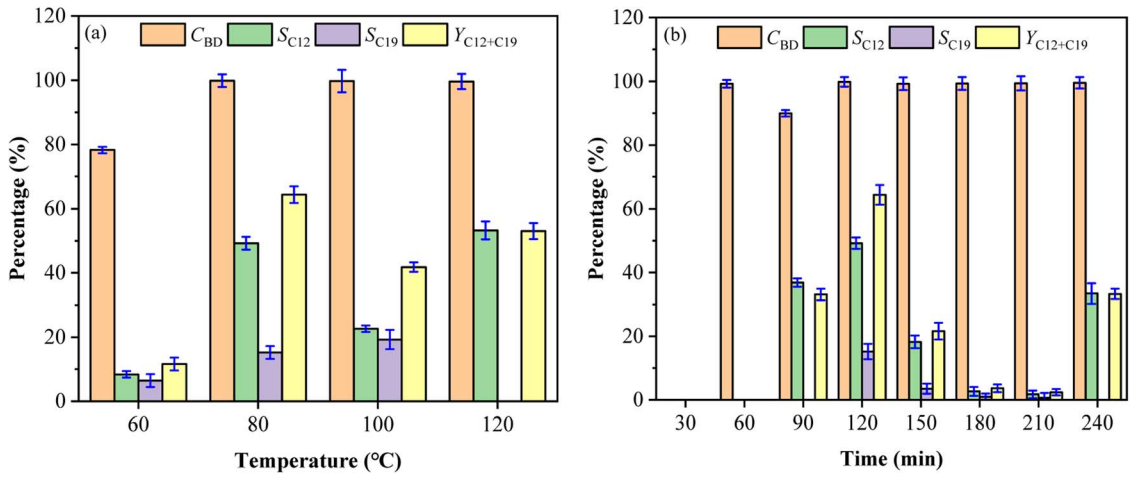

Fig. 3 Production of C12 and C19 precursors under different (a) temperatures and (b) time (BD : CPO = 1 : 6, ChCl : Fa = 1 : 12, 4 mmol $SnCl_4$).

(99.18% and 99.25%, respectively) when the condensation time was 30 min and 60 min, which demonstrated that the selective condensation of C12 and C19 cannot be satisfied in shorter reaction time. BD and CPO were condensed to form C12 (S_{C12} was 36.82%) but not C19 when the reaction time was 90 min while the C12 and C19 were successfully condensed when the time was 120 min. This illustrated that the time required for the condensation to C12 was shorter than that of C19, and the time cost could be reduced by a reasonable adjustment of the condensation time of the two. However, the selectivity and the total yield of C12 and C19 were greatly reduced after 120 min (from 150 min to 240 min). The S_{C12}, S_{C19} and $Y_{C12+C19}$ at 150 min were 18.25%, 3.53% and 21.62% respectively, while the $Y_{C12+C19}$ at 180 min and 210 min were only 3.64% and 2.41% respectively. It showed that the reaction time exceeding 120 min was unfavorable for the selective condensation of C12 and C19 in the catalytic system, which may be due to the excessively long condensation time leaded to the further non-targeted conversions of the generated C12 and C19, and decreased its selectivity and total yield. In summary, 80 °C and 120 min were chosen as the optimum condensation temperature and time in this work for the A–K condensation of BD and CPO in ChCl/Fa–$SnCl_4$ system.

Effect of molar ratio of DES and substrates on fuel precursors

The selectivity and total yield of C12 and C19 first increased and then decreased with the decrease of the ChCl and Fa molar ratios (the content of Fa increased), while the change of molar ratios had little effect on C_{BD} with the higher values (nearly 100%) at different molar ratios as shown in Fig. 4a. S_{C12}, S_{C19} and $Y_{C12+C19}$ were reduced by 4.21%, 8.87% and 12.63% respectively at ChCl : Fa molar ratio of 1 : 4, while the values increased to 18.51%, 10.05% and 28.46% respectively at ChCl : Fa molar ratio of 1 : 8 and the maximum values were obtained at ChCl : Fa molar ratio of 1 : 12 (49.2%, 15.2% and 64.37%). This indicated that the enhancement of acidity in DES system could improve the condensation process of BD and CPO to a certain extent, which was a primary reason. However, the underlying reason lied in the hydrogen bonds formed between ChCl and Fa. The acidic environment provided by Fa made the generation of hydrogen bonds easier, thereby reducing the melting point of ChCl/Fa. The presence of hydrogen bonds led to the system become more stable compared with the common reaction system,[22] and thus facilitated the formation of C12 and C19 with a higher selectivity. The increase of Fa, however, was limited to a certain extent. For example, the selectivity of C12 and C19 decreased significantly when the molar ratios of ChCl/Fa decreased from 1 : 16 to 1 : 20. S_{C12}, S_{C19} and Y_{C12+C1} were 5.36%, 1.28%, and 6.62% respectively at ChCl : Fa molar ratio of 1 : 16, and the values were 3.76%, 1.02% and 4.76% respectively at ChCl : Fa molar ratio of 1 : 20. This may be due to the excess of Fa made too much H^+ ions in the system making it unable to generate hydrogen bonds with ChCl, which undermined the stability of the ChCl/Fa system.[21] Moreover, the acidity of the system exceeded the acidity range that the substrates can withstand in the condensation reaction, resulting in the selective inhibition condensation of C12 and C19.

The molar ratios of BD and CPO had little influence on C_{BD}, while the significant influence on S_{C12}, S_{C19} and $Y_{C12+C19}$ was observed as shown in Fig. 4b. The values of S_{C12} and S_{C19} first increased and then decreased as the molar ratio of BD and CPO increased from 1 : 3 to 1 : 12, and the maximum value was reached at BD : CPO molar ratio of 1 : 6 while C12 and C19 were not condensed at BD : CPO molar ratio of 1 : 12. It can be seen that too low or excessive proportion of CPO would have a significant impact on the yield of the fuel precursors. This phenomenon probably because that C12 and C19 cannot be directionally condensed when the ratio of cyclopentanone was insufficient, although BD had a high conversion in the condensation process. Furthermore, the coordination strength between $SnCl_4$ and the carbonyl group of CPO may be strengthened when CPO was in excess,[19] and the more enol precursors formed, the further converted the originally formed compounds into other non-directional by-products. The accessibility of BD and CPO condensation to form C12 and C19 precursors was greatly reduced due to the relatively low content

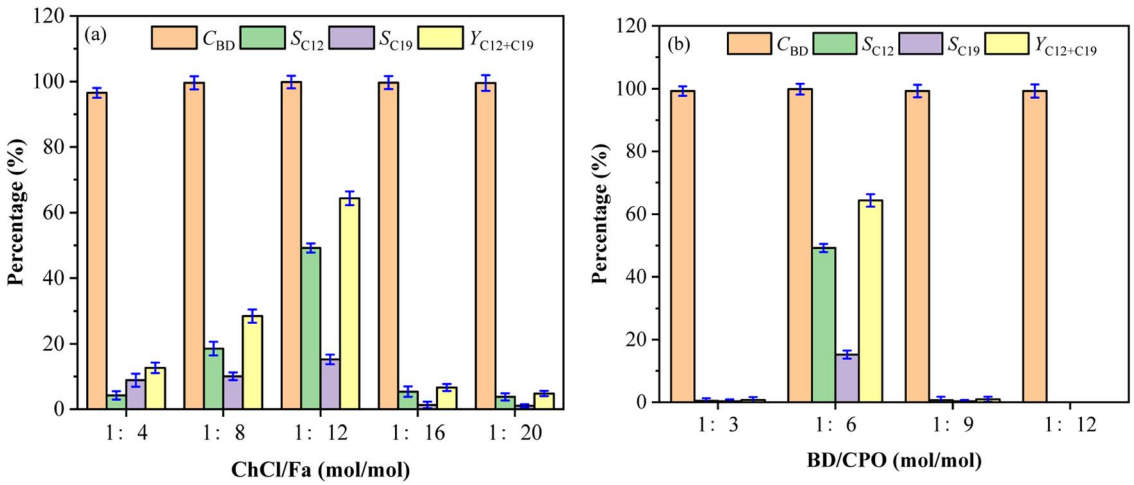

Fig. 4 Production of C12 and C19 precursors under different molar ratios of (a) ChCl/Fa and (b) BD/CPO (4 mmol $SnCl_4$, 80 °C for 120 min).

of BD. To sum up, the optimal molar ratios of ChCl : Fa and BD : CPO in this catalytic system were 1 : 12 and 1 : 6, respectively.

Effect of $SnCl_4$ loadings on fuel precursors

Fig. 5 showed the effect of $SnCl_4$ loadings on the formation of C12 and C19 precursors in this system. As the increase of $SnCl_4$ loadings from 0 mmol to 6 mmol, the selectivity of C12 and C19 increased first and then decreased, but had no obvious effect on the conversion of BD. There was no condensation to generate C12 with $SnCl_4$ not added, which possibly because of the absence of $SnCl_4$ weakened the directional regulation of the condensation process. It cannot inhibit the directional and non-directional transformation of C12 that further condensed into C19 and other by-products. The maximum values of S_{C12}, S_{C19} and $Y_{C12+C19}$ were obtained at 4 mmol $SnCl_4$ loading and the values decreased significantly with increasing 6 mmol $SnCl_4$, which manifested excessive $SnCl_4$ may inhibit the condensation of BD and CPO owing to the potential recrystallisation process between $SnCl_4$ and ChCl[36] or promote the conversion of C12 and C19 to other compounds.

Based on the investigation on the process of synthesizing fuel precursors C12 and C19 by A–K condensation of BD and CPO in ChCl/Fa–$SnCl_4$ system, the optimal conditions for the condensation process in this work were ultimately determined: the molar ratio of BD : CPO molar ratio of 1 : 6 and ChCl : Fa molar ratio of 1 : 12, 4 mmol $SnCl_4$, 80 °C for 120 min, the conversion of BD was 99.96%, the selectivity and total yield of C12 and C19 were 49.20%, 15.20% and 64.37% respectively.

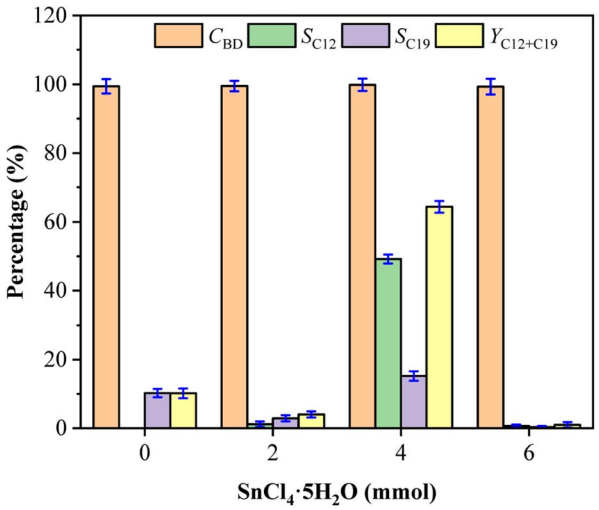

Fig. 5 Production of C12 and C19 precursors under different loadings of $SnCl_4$ (BD : CPO molar ratio of 1 : 6, ChCl : Fa molar ratio of 1 : 12, 80 °C for 120 min).

Production of cyclic alkane fuels from fuel precursors by HDO

The C12 and C19 fuel precursors obtained under the optimal conditions were further applied to produce cyclic alkane fuels by HDO. The GS-MS analysis of the HDO products showed that the corresponding cyclic alkanes ($C_{12}H_{14}$ and $C_{19}H_{18}$) were formed after HDO of C12 and C19 precursors (as shown in Fig. 6). $C_{12}H_{14}$ was obtained with the selectivity of 37.61% and total yield of 18.50%, and the selectivity and the total yield of $C_{19}H_{18}$ was 24.10% and 3.67% respectively. The feasibility of further conversion of the fuel precursors to cyclic alkane fuels was realized by the elimination of the oxygen-containing groups in the fuel precursors after HDO. However, the cyclic alkanes obtained in this work were still unsaturated alkanes with low saturation. This may be due to the insufficient hydrogen source provided to the reaction system by MAPR,[23] resulting in the inability of the unsaturated C=C bonds in the alkanes to continue to be broken and hydrogenated to generate saturated alkane fuels. Besides, it may also depend on the loadings of catalysts and the degree of reaction (temperature and/or time) in HDO process, which need to be further investigated in future work.

Mechanism of BD and CPO condensation in ChCl/Fa–$SnCl_4$ system

DFT calculations were implemented to investigate the A–K condensation process of BD and CPO into C12 and C19 precursors in ChCl/Fa–$SnCl_4$ catalytic system. All optimized geometries were visually presented in Fig. 7, and the total energy (TE), dielectric energy (DE), zero point vibrational energy (ZPVE) and exchange correlation (EC) of these geometries were shown in Table 2. The TE, DE and ZPVE of DES ChCl/Fa (−1024.41 Ha, −51.44 kcal mol^{-1} and 145.48 kcal mol^{-1}, respectively) were observed to be significantly higher than its HBA (ChCl) and HBD (Fa), which might be attributed to the classic hydrogen bonds (–N–H···Cl) formed between ChCl and Fa resulting in the DES being a stable system with high catalytic

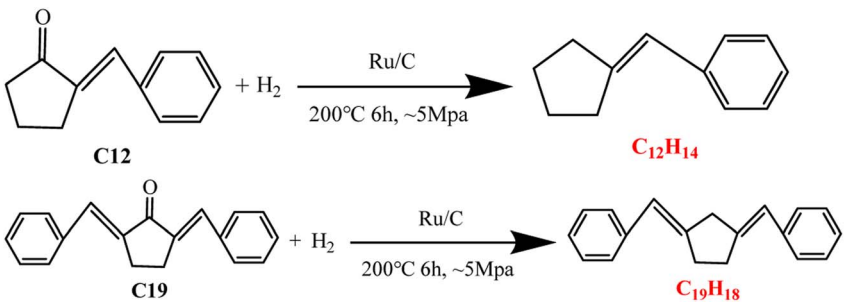

Fig. 6 HDO of C12 and C19 precursors to form cyclic alkanes.

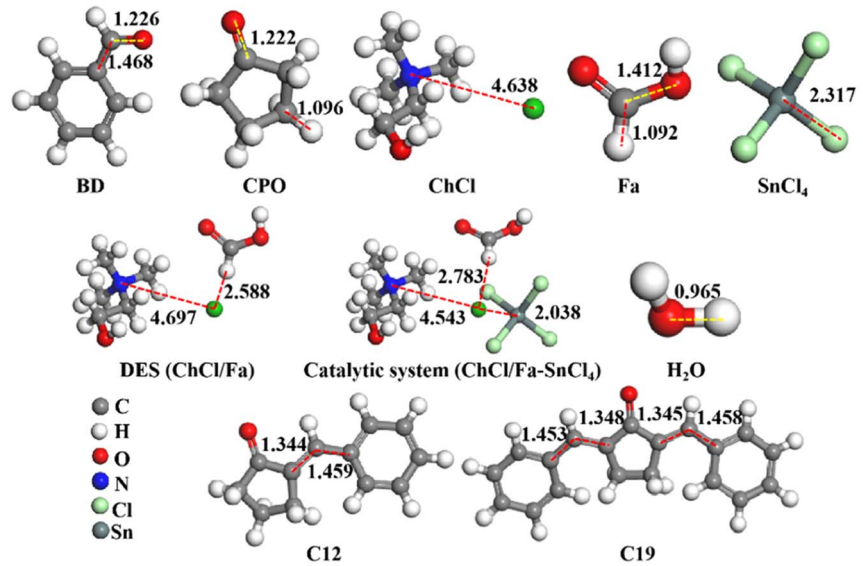

Fig. 7 Optimized structures of reactants (BD and CPO), DES ChCl/Fa, $SnCl_4$, ChCl/Fa–$SnCl_4$ and products (C12, C19 and H_2O).

Table 2 TE, DE, ZPVE and EC of optimized structures

Structures	TE (Ha)	DE (kcal mol^{-1})	ZPVE (kcal mol^{-1})	EC (Ha)
BD	−366.81	−7.20	69.11	0.62
CPO	−286.83	−10.92	76.33	0.77
ChCl	−824.21	−64.92	123.99	1.01
Fa	−200.32	−6.74	21.11	0.30
$SnCl_4$	−8024.06	−1.90	2.75	0.18
ChCl/Fa	−1024.41	−51.44	145.48	1.31
ChCl/Fa–$SnCl_4$	−9048.69	−56.73	149.23	1.50
C12	−572.95	−20.67	131.21	1.17
C19	−859.15	−28.30	185.35	1.70

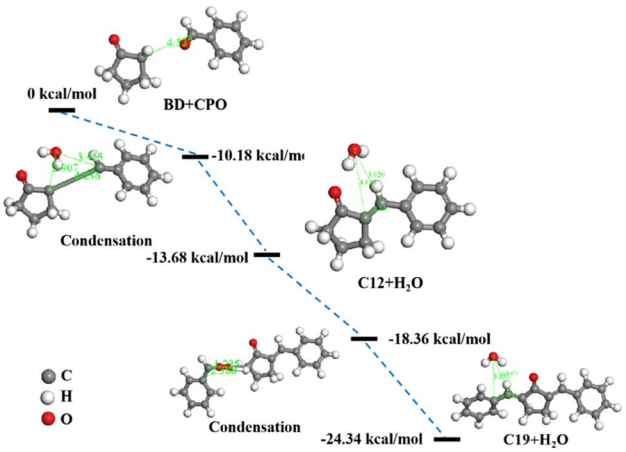

Fig. 8 Energy barriers profile by transition state search in DMol^3 module with schematic geometries of condensation routes.

capability.[38] Compared to DES ChCl/Fa, the catalytic system ChCl/Fa–$SnCl_4$ was found to be a more robust structure with TE, DE and ZPVE of −9048.69 Ha, −56.73 kcal mol^{-1} and 149.23 kcal mol^{-1}, respectively due to the feasible interaction structures among the ChCl, Fa and $SnCl_4$, which were primarily formed by coordination bonds, electrostatic interactions and H-bonds.[38,39] A charge transfer was conducted from chloride ion (Cl^-) to choline ion (Ch^+) in DES and tin ion (Sn^{4+}) in $SnCl_4$.[38] The coupling Cl^- in ChCl and H^+ in Fa was capable of forming a strong H-bond (H···Cl) similar to hydrogen chloride. The coordination bonds were formed between the Cl^- in ChCl and Sn^{4+} in $SnCl_4$.[40–42] The catalytic system ChCl/Fa–$SnCl_4$ with reliable structure can reduce reaction energy barriers to promote A–K condensation of BD and CPO.

Fig. 8 showed the energy barriers calculated by transition state search in DMol^3 module of BD and CPO condensation reactions and the condensation routes. The reaction energy barriers progressively increased as the condensation of BD and CPO into C12 and C19 fuel precursors, which demonstrated that C12 and C19 were structurally steady and resistant to further condensation. C12 was first performed with an energy barrier of −13.68 kcal mol^{-1} by the condensation of the carbon on aldehyde group of BD and the carbon near carbonyl group of CPO to develop a C=C bond and remove a H_2O molecule with an energy barrier of −10.18 kcal mol^{-1}. Then, C12 and BD continued to condense to form C19 with the energy barrier of −24.34 kcal mol^{-1} through the incorporation of the carbon on aldehyde group of BD and the carbon on five-membered ring of C12 (C–C bond) similarly removing a H_2O with the energy barrier of −18.36 kcal mol^{-1}. The length of C=C bonds (1.344 Å and 1.453, respectively) formed in C12 and C19 was less than the length of the C–C bonds before condensation, indicating the reduced reactivity of C12 and C19 compared to BD and CPO. The results can also be elucidated by the high TE, DE and ZPVE values of C12 (−572.95 Ha, −20.67 kcal mol^{-1} and 131.21 kcal mol^{-1}, respectively) and C19 (−859.15 Ha, −28.30 kcal mol^{-1} and 185.35 kcal mol^{-1}, respectively) shown in Table 1.

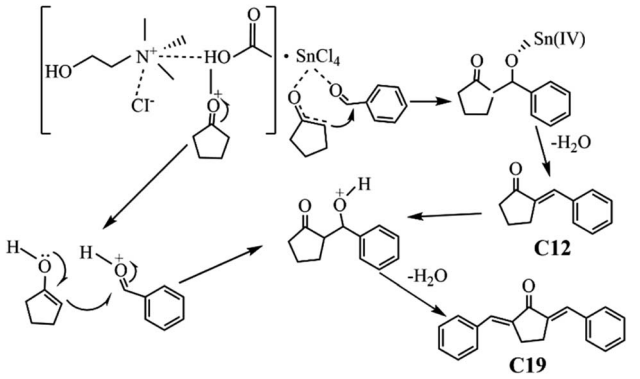

Fig. 9 Condensation mechanism of BD and CPO in ChCl/Fa–$SnCl_4$ system.

The plausible condensation mechanism of BD and CPO in ChCl/Fa–$SnCl_4$ catalytic system was depicted in Fig. 9. The condensation of BD and CPO was the synergistic effect of ChCl/Fa and $SnCl_4$. The carbonyl group (C=O) on CPO was first attacked by Sn^{4+} in $SnCl_4$ and protonated to form the carbon cation with electron-deficient intermediates, and then the intermediates formed an enol structure containing a C=C bond through coordination and removed a H_2O molecular.[36] Simultaneously, the aldehyde group (H–C=O) on BD was attacked and activated by $COOH^-$ in Fa and then protonated resulting in protons release and electrons transfer during the dehydration process.[40] The chemical bonds of BD and CPO were rapidly broken under synergistic catalysis to accelerated the dehydration and condensation process, which fabricated the primary product C12 precursor. The protonated carbonyl group in C12 continued to undergo electrons transfer in the catalytic system to form an enol structure with a C=C bond which then reacted with BD to develop the secondary product C19 precursor. In the DES ChCl/Fa, the presence of strong H-bonds facilitated the condensation of BD and CPO into fuel precursors.[43] Moreover, the acidic environment provided by Fa might have a positive effect on enhancing the catalytic behavior of Sn^{4+} and $COOH^-$.[29,31,44] However, the anions (Cl^-, $COOH^-$) would have stronger interactions with Sn^{4+}, competing with the interaction between BD and Sn^{4+} and inhibiting the development of fuel precursors. Hu *et al.* found that some anions (Cl^-, Tf_2N^-, TFA^-, *etc.*) in ionic liquids could interact vigorously with Sn^{4+} to form pentacyclic chelates, which would rival with the interaction between glucose and Sn^{4+} and thus suppress the conversion of glucose into HMF when using $SnCl_4$ and ionic liquids as catalytic system.[32] The cooperation of DES and Sn^{4+} could also be illustrated by far-infrared spectroscopic characterization of $SnCl_4$ based on previous work.[37] The peak of $SnCl_4$ in the DES became sharp, and the absorption peak of Sn–Cl decreased in absorbance compared to the metal–Cl bond with an intense stretching vibration of the absorption band around 300 cm^{-1}.[45] Furthermore, the absorbance of $SnCl_4$ in the DES decreased more greatly due to the coordination of Sn^{4+} with the carbonyl group, which indicated an enhancement of the catalytic reaction.

Conclusion

In this work, the fuel precursors C12 and C19 were successfully synthesized by aldehyde–ketone condensation of BD and CPO in ChCl/Fa–$SnCl_4$ catalytic system. The high selectivity and total yield of C12 and C19 (49.20%, 15.20% and 64.37%) were obtained under the optimal conditions of BD : CPO molar ratio of 1 : 6, ChCl : Fa molar ratio of 1 : 12, 4 mmol $SnCl_4$, 80 °C for 120 min. The further HDO of C12 and C19 precursors was performed to form cyclic alkane fuels $C_{12}H_{14}$ and $C_{19}H_{18}$ with the total yield of 18.50% and 3.67% respectively. DFT results revealed that the presence of hydrogen and coordination bonds between ChCl/Fa and $SnCl_4$ played a pivotal role in forming the desirable ChCl/Fa–$SnCl_4$ system with a steadfast structure, which resulted in lower reaction energy barriers to encourage the condensation process of BD and CPO. The condensation of BD and CPO into C12 and C19 was the consequence of synergistic catalysis by DES and $SnCl_4$. The ChCl/Fa–$SnCl_4$ catalytic system was proven to be beneficial for the synthesis of biofuel precursors with high selectivity and carbon chain length under mild conditions. The findings of this work open up an effective and practicable avenue for the catalytic synthesis of sustainable liquid biofuels. However, the recovery and reusability of DES in the catalytic system are an important challenge and research direction for the future research.

Data availability

The data used in this work can be made available upon reasonable request to the corresponding author.

Author contributions

Yunqi Cao: conceptualization, methodology, formal analysis, writing – original draft. Fang Liu: resources, writing – review and editing, supervision. Yunyun Liu: conceptualization, investigation, funding acquisition, writing – review and editing. Qiang Yu: supervision, writing – review and editing, funding acquisition.

Conflicts of interest

The authors declare that they have no known competing financial interests or personal relationships that could have appeared to influence the work reported in this paper.

Acknowledgements

This work was financially supported by the Basic Research Program of Natural Sciences in Shaanxi Province (2021JM-382) and the National Natural Science Foundation of China (51876206).

References

1 K. T. T. Amesho, Y.-C. Lin, S. V. Mohan, S. Halder, V. K. Ponnusamy and S.-R. Jhang, *Environ. Chem. Lett.*, 2023, **21**, 183–230.

2 N. S. Ab Rasid, A. Shamjuddin, A. Z. Abdul Rahman and N. A. S. Amin, *J. Cleaner Prod.*, 2021, **321**, 129038.
3 X. Zhang, P. Zhu, Q. Li and H. Xia, *Front. Chem.*, 2022, **10**, 911674.
4 J. Ma, S. Shi, X. Jia, F. Xia, H. Ma, J. Gao and J. Xu, *J. Energy Chem.*, 2019, **36**, 74–86.
5 W. Wang, X. Zhang, Z. Jiang, Y. Cui, Q. Kang, X. Zhao, Q. Zhang and L. Ma, *Fuel*, 2022, **321**, 124114.
6 P. Juárez, C. López-Aguado, M. Paniagua, J. A. Melero, R. Mariscal and G. Morales, *Appl. Catal., A*, 2022, **631**, 118480.
7 Z. Li, Q. Li, Y. Wang, J. Zhang and H. Wang, *Energy Fuels*, 2021, **35**, 6691–6699.
8 X. Shang, Y. Yang and Y. Sun, *Green Chem.*, 2020, **22**, 5395–5401.
9 H. Gao, F. Han, G. Li, A. Wang, Y. Cong, Z. Li, W. Wang and N. Li, *Sustainable Energy Fuels*, 2022, **6**, 1616–1624.
10 W. Wang, X. Ji, H. Ge, Z. Li, G. Tian, X. Shao and Q. Zhang, *RSC Adv.*, 2017, **7**, 16901–16907.
11 Z. Li, L. Pan, G. Nie, J. Xie, J. Xie, X. Zhang, L. Wang and J.-J. Zou, *Chem. Eng. Sci.*, 2018, **191**, 343–349.
12 Y. Jing, Q. Xia, X. Liu and Y. Wang, *ChemSusChem*, 2017, **10**, 4817–4823.
13 Y. B. Huang, X. Y. Yan, Z. H. Huang, T. X. Shan, J. Y. Geng, Z. H. Cao and Q. Lu, *ChemSusChem*, 2022, e202201677.
14 Q. Xia, Z. Chen, Y. Shao, X. Gong, H. Wang, X. Liu, S. F. Parker, X. Han, S. Yang and Y. Wang, *Nat. Commun.*, 2016, **7**, 11162.
15 J. He, Q. Qiang, S. Liu, K. Song, X. Zhou, J. Guo, B. Zhang and C. Li, *Fuel*, 2021, **306**, 121765.
16 J. Anibal and B. Xu, *ACS Catal.*, 2020, **10**, 11643–11653.
17 Y.-B. Huang, Z. Yang, J.-J. Dai, Q.-X. Guo and Y. Fu, *RSC Adv.*, 2012, **2**, 11211–11214.
18 Y. Wang, D. Hu, R. Guo, H. Deng, M. Amer, Z. Zhao, H. Xu and K. Yan, *Mol. Catal.*, 2022, **528**, 112505.
19 Y. Jing, Y. Xin, Y. Guo, X. Liu and Y. Wang, *Chin. J. Catal.*, 2019, **40**, 1168–1177.
20 L. Smoláková, L. Dubnová, J. Kocík, J. Endres, S. Daniš, P. Priecel and L. Čapek, *Appl. Clay Sci.*, 2018, **157**, 8–18.
21 N. Sun, C. Gong, Y. Zhou, Y. Zhang, N. Zhang, L. Xing and W. Xue, *ACS Omega*, 2023, **8**, 2556–2563.
22 Z. Li, S. Shao, X. Hu, X. Li and Y. Cai, *Biomass Convers. Biorefin.*, 2022, 1–12.
23 J. Gupta, K. Papadikis, E. Y. Konysheva, Y. Lin, I. V. Kozhevnikov and J. Li, *Appl. Catal., B*, 2021, **285**, 119858.
24 W. Li, M. Su, T. Zhang, Q. Ma and W. Fan, *Fuel*, 2019, **237**, 1281–1290.
25 M. Xu, S. Célérier, J.-D. Comparot, J. Rousseau, M. Corbet, F. Richard and J.-M. Clacens, *Catal. Sci. Technol.*, 2019, **9**, 5793–5802.
26 L. Chen, Y. Xiong, H. Qin and Z. Qi, *ChemSusChem*, 2022, **15**, e202102635.
27 B. Chen, Z. Peng, C. Li, Y. Feng, Y. Sun, X. Tang, X. Zeng and L. Lin, *ChemSusChem*, 2021, **14**, 1496–1506.
28 R. K. Ibrahim, M. Hayyan, M. A. AlSaadi, S. Ibrahim, A. Hayyan and M. A. Hashim, *J. Mol. Liq.*, 2019, **276**, 794–800.
29 S. Hong, X.-J. Shen, Z. Sun and T.-Q. Yuan, *Front. Energy Res.*, 2020, **8**, 57198.
30 H. Ji and P. Lv, *Green Chem.*, 2020, **22**, 1378–1387.
31 R. Gautam, N. Kumar and J. G. Lynam, *J. Mol. Struct.*, 2020, **1222**, 128849.
32 S. Hu, Z. Zhang, J. Song, Y. Zhou and B. Han, *Green Chem.*, 2009, **11**, 1749.
33 H. Li, Z. Xu, P. Yan and Z. C. Zhang, *Green Chem.*, 2017, **19**, 1751–1756.
34 X. Guo, H. Zhu, Y. Si, X. Lyu, Y. Cheng, L. Zheng, L. Wang and X. Li, *Ind. Eng. Chem. Res.*, 2022, **61**, 7216–7224.
35 K. Wang, A. Rezayan, L. Si, Y. Zhang, R. Nie, T. Lu, J. Wang and C. Xu, *ACS Sustain. Chem. Eng.*, 2021, **9**, 11351–11360.
36 Q. Yu, R. Bai, F. Wang, Q. Zhang, Y. Sun, Y. Zhang, L. Qin, Z. Wang and Z. Yuan, *J. Chem. Technol. Biotechnol.*, 2019, **95**, 751–757.
37 Y. Liu, Y. Wang, Y. Cao, X. Chen, Q. Yu, Z. Wang and Z. Yuan, *ACS Sustain. Chem. Eng.*, 2020, **8**, 6949–6955.
38 D. K. Mishra, G. Gopakumar, G. Pugazhenthi, C. V. Siva Brahmmananda Rao, S. Nagarajan and T. Banerjee, *J. Phys. Chem. A*, 2021, **125**, 9680–9690.
39 J. Zhang, C. Yang, F. Niu, S. Gao and J. Dong, *Minerals*, 2021, **11**, 1080.
40 L. Zhou, X. Lu, Z. Ju, B. Liu, H. Yao, J. Xu, Q. Zhou, Y. Hu and S. Zhang, *Green Chem.*, 2019, **21**, 897–906.
41 K. Essalah, M. A. Sanhoury, M. T. Ben Dhia, M. Abderrabba and M. R. Khaddar, *J. Mol. Struct.: THEOCHEM*, 2010, **942**, 110–114.
42 M. T. Ben Dhia, M. A. M. K. Sanhoury, L. C. Owono Owono and M. R. Khaddar, *J. Mol. Struct.*, 2008, **892**, 103–109.
43 Q. Yu, Z. Song, X. Zhuang, L. Liu, W. Qiu, J. Shi, W. Wang, Y. Li, Z. Wang and Z. Yuan, *Cellulose*, 2019, **26**, 8263–8277.
44 M. Zuo, X. Wang, Q. Wang, X. Zeng and L. Lin, *ChemSusChem*, 2022, **15**, e202101889.
45 H. Li and Z. C. Zhang, *Chin. J. Catal.*, 2016, **37**, 637–643.